

Enantioselective Synthesis of Pyrrolidines by Imidodiphosphorimidate (IDPi)-Catalysed *anti*-selective Hydroamination of Alkenes

Sudip Guria¹, Alexander N. Volkov^{2,3}, Raffi Khudaverdyan¹, Ruben Van Lommel⁴, Constantin G. Daniliuc⁵, Frank De Proft⁴ and Ulrich Hennecke^{1*}

¹ Organic Chemistry Research Group, Department of Chemistry and Department of Bioengineering Sciences, Vrije Universiteit Brussel (VUB), Pleinlaan 2, 1050 Brussels, Belgium; ² VIB Centre for Structural Biology, Vlaams Instituut voor Biotechnologie (VIB), Pleinlaan 2, Brussels 1050, Belgium; ³ Jean Jeener NMR Centre, Vrije Universiteit Brussel (VUB), Pleinlaan 2, Brussels 1050, Belgium; ⁴ General Chemistry Research Group, Department of Chemistry, Vrije Universiteit Brussel (VUB), Pleinlaan 2, 1050 Brussels, Belgium; ⁵ Organisch-Chemisches Institut, University of Münster, Corrensstr. 40, 48149 Münster, Germany

Chiral pyrrolidines are common structural motives in natural products as well as active pharmaceutical ingredients explaining the need for methods for their enantioselective synthesis. While several, often metal-catalyzed, methods do exist, the enantioselective synthesis of pyrrolidines containing quaternary stereocentres remains challenging. Herein, we report a Brønsted acid-catalysed intramolecular hydroamination, which provides such pyrrolidines from simple starting materials in high yield and enantioselectivity. Key to an efficient reaction was the use of an electron-deficient protective group on nitrogen, the common nosyl protecting group, to avoid deactivation of the Brønsted acid by deprotonation. The reaction proceeds as a stereospecific anti-addition indicating a concerted reaction. Furthermore, kinetic studies show Michaelis-Menten behaviour suggesting the formation of a precomplex similar to those observed in enzymatic catalysis.

Nitrogen-containing heterocycles are prevalent motives in natural products and active pharmaceutical ingredients (APIs) (Figure 1A).^{1,2} However, while chiral saturated heterocycles rich in sp³-hybridised carbon atoms are predominant in natural products, planar aromatic heterocycles are more commonly found in drugs. This has been identified as a possible problem in drug development and the use of more saturated heterocycles has been recommended.³ The most common saturated nitrogen heterocycles in APIs are pyrrolidines,⁴ which have also found many applications as organocatalysts and ligands for transition metal catalysts.^{5,6} Due to the ubiquitous presence of nitrogen-containing chiral heterocycles, developing synthetic methods for their preparation has always been an important topic in organic chemistry.^{1,7} Intramolecular hydroamination of alkenes is an attractive strategy for the synthesis of saturated nitrogen-containing heterocycles proceeding with full atom economy. Over the last three decades, enantioselective hydroamination of alkenes has been chiefly carried out using metal catalysis, enabling both intermolecular and intramolecular reactions.^{8,9} However, intramolecular hydroaminations of highly substituted alkenes to provide saturated heterocycles remain challenging using transition metal catalysis. Alternatively, hydroamination can also be carried out via radical chemistry¹⁰, photoredox catalysis^{11,12} or Brønsted acid catalysis.^{13,14} In these cases, achieving high enantioinduction is difficult, although anti-Markovnikov hydroamination to form pyrrolidines with high enantioselectivity was recently achieved via proton-coupled electron transfer (PCET).¹⁵ Furthermore, the use of chiral Brønsted acids provides an additional challenge: the acid needs to be acidic enough to protonate the alkene without being deactivated (deprotonated) by the amine-containing starting materials or products.^{13,14} Jacobsen circumvented this problem by using hydroxylamines as substrates, which react in intramolecular hydroamination via a retro-Cope-type mechanism under thiourea catalysis to give pyrrolidines.¹⁶ Asymmetric, Brønsted acid-catalyzed hydroamination has also been reported for more reactive/easier to protonate unsaturated groups such as allenes and conjugated dienes.^{17,18} In 2008, the Ackermann group reported a first enantioselective hydroamination of an alkene by a basic amine using a chiral phosphoric acid diester catalyst providing a pyrrolidine with 17% *ee* (Figure 1B).¹⁹ Significantly improved enantioselectivity in Brønsted acid-catalyzed hydroamination was reported by Tan and Liu when a thiourea group

was installed on the nitrogen atom.²⁰⁻²² However, in both cases geminal disubstitution of the starting materials causing a Thorpe-Ingold effect²³ was required to achieve efficient and enantioselective reactions. Considering the limited substrate scope of current asymmetric Brønsted acid-catalyzed hydroamination and their requirements of non-standard protective groups, we reasoned that the application of List's new generation of chiral Brønsted acids such as imididiphosphate (IDPs)²⁴ or imidodiphosphorimidates (IDPis)²⁵ could solve these issues. These Brønsted acids provide a more confined environment and, in the case of the IDPis, a significantly higher acidity which proved very beneficial for alkene hydroalkoxylation.²⁶ However, as discussed above, it is not certain that the higher acidity can be useful in hydroaminations as the interaction with the basic nitrogen atom can lead to catalyst deactivation. In this work we show that IDPis, when combined with a suitable protecting group on nitrogen such as a nosyl group enable highly enantioselective intramolecular hydroaminations on a broad scope of substrates (Figure 1C). Mechanistic studies demonstrate that the reaction proceeds with high *anti*-diastereoselectivity placing the proton and the nucleophile on opposite sides of the alkene implying a concerted addition.

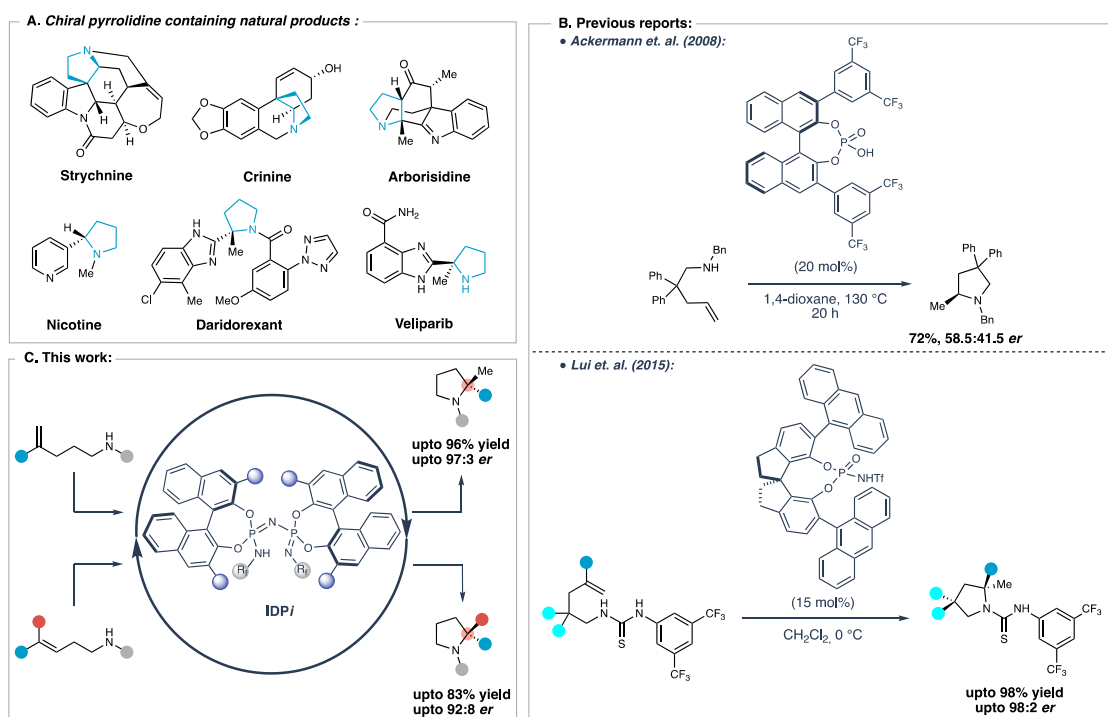


Figure 1: A. Pyrrolidine-containing alkaloids and APIs; B. Previous work on asymmetric Brønsted acid-catalyzed hydroamination; C. Envisioned hydroamination catalyzed by IDPis.

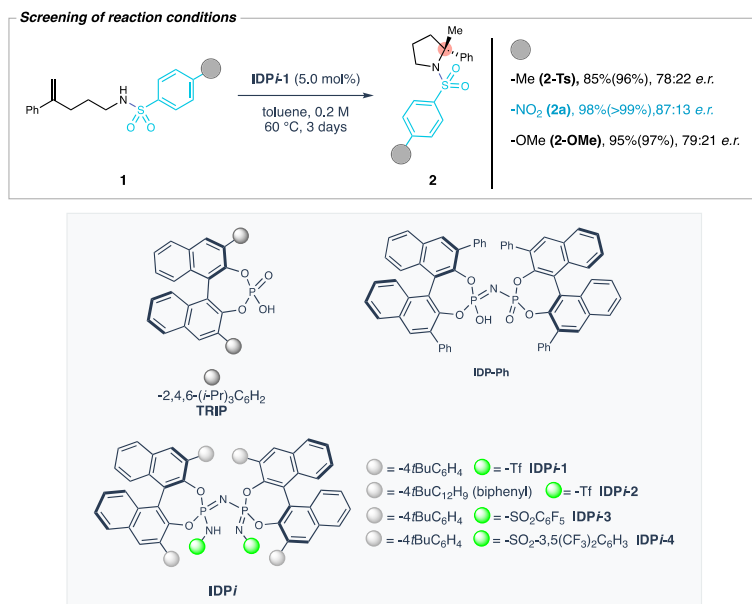
Results

Reaction development

In the first step, the 5-*exo* cyclization of acyclic 1,1-disubstituted sulfonamides **1** to form chiral pyrrolidine derivatives **2** was investigated. Initial experiments had shown that sulfonyl protection of nitrogen with a tosyl group enabled intramolecular hydroamination catalyzed by **IDPi-1** to obtain **2-Ts** in good yield (85%) and a reasonable enantioselectivity (78:22 *er*; Tab. 1). Replacing the tosyl protecting group by a more electron-deficient nosyl group improved the yield and the enantioselectivity (87:13 *er*) significantly, whereas a methoxyphenyl-substituted sulfonamide had no effect on selectivity. Further improvement could be achieved by the optimisation of the catalyst structure. While less acidic catalysts such **TRIP** and **IDP-Ph** were either not able to catalyze the reaction at all, or only led to low conversion, **IDPi**-type catalysts in general performed well and provided acceptable conversion. Major differences, however, were observed concerning the enantioselectivity of the reaction. Changing the 3,3'-substituents on the BINOL backbone from 4-*tert*-butylphenyl (**IDPi-1**) to biphenyl (**IDPi-2**) caused a complete loss of enantioselectivity. Altering the substituent on the catalyst's sulfonamide had

less influence on the enantioselectivity, but **IDPi-4** was less reactive than other **IDPis** (37% conversion) which excluded further optimisation with this catalyst despite showing excellent enantioselectivity. Instead, excellent reaction conditions with **IDPi-3** were achieved when lowering the reaction temperature to 40 °C and optimisation of the reaction concentration, which provided the reaction product in 99% yield (94% isolated yield) and in excellent enantioselectivity of 97:3 *er* (table 1, entry 10).

Table 1: Optimization for 1,1-disubstituted alkene derivative(s):



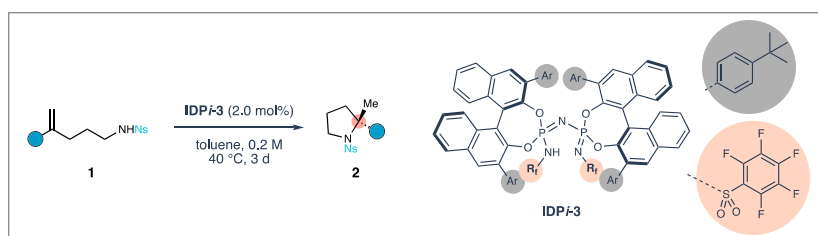
entry	catalyst	temperature (°C)	conversion (%)	Yield 2a (%) ^a	<i>er</i> (2a) ^b
1	TRIP	60	no reaction	-	-
2	IDP-Ph	60	18	11	68:32
3	IDPi-1	60	>99	98	87:13
4	IDPi-2	60	>99	97	51:49
5	IDPi-3	60	>99	92	84:16
6	IDPi-4	60	37	33	96:4
7	IDPi-1	50	79	78	94:6
8	IDPi-3	50	>99	99	96:4
9	IDPi-4	80	93	78	94:6
10 ^c	IDPi-3	40	>99	99(94 ^d)	97:3

Reaction Conditions: **1a** (0.1 mmol), catalyst (0.005 mmol) in 0.5 mL toluene at the mentioned temperature under the argon atmosphere for 3 days. ^a NMR yield using dimethyl terephthalate as the internal standard. ^b *er* was determined by HPLC using a chiral stationary phase. ^c The reaction was performed using 2.0 mol% **IDPi-3** and 0.3 mmol scale **1a**. ^d Isolated yield.

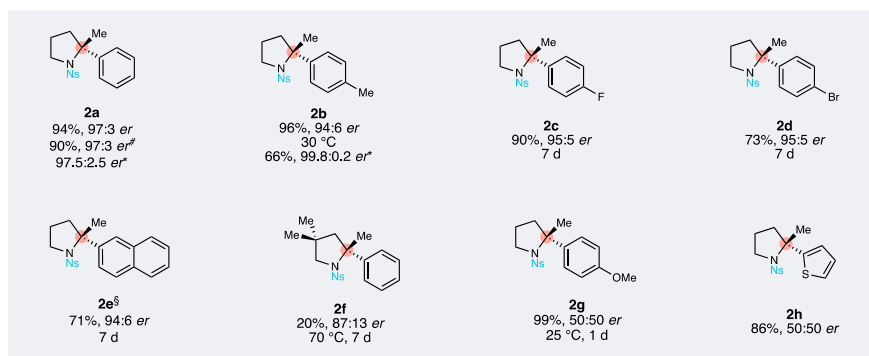
Scope of the reaction

The newly developed reaction conditions were applied to a range of 1,1-disubstituted alkenes **1** and proved a high substrate generality providing showing enantioselectivity in most cases (Scheme 1). Several different substituents such as -Me, -Br and -F were tolerated at the *para*-position of the starting material's phenyl group. Yields (73-96%) and enantioselectivity (94:6 and 95:5 *er*) remained high and quite comparable for these starting materials. Cyclization of 2-naphthyl-substituted **1e** required a slightly higher catalyst loading providing the product **2e** in good yield (71%) and high enantioselectivity (94:6 *er*), however, a 1-naphthyl substituted starting material was unreactive (see supporting information). Geminal disubstitution of the chain also reduced the

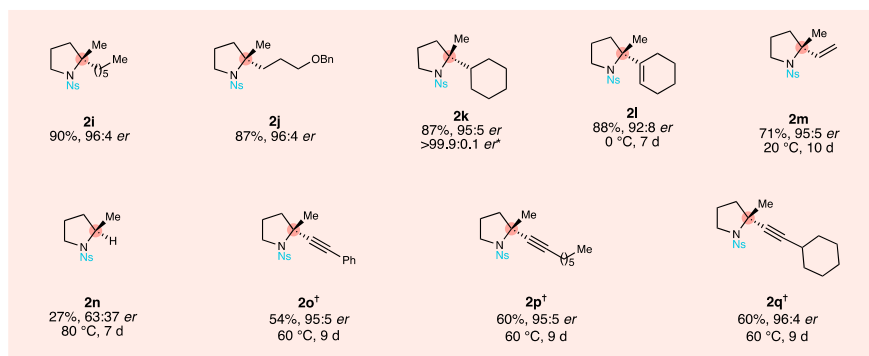
reactivity of starting material **1f**, but the product **2f** was still formed in good selectivity (87:13 *er*) albeit in low yield (20%). Compared to related hydroaminations, a potential Thorpe-Ingold effect²³ does not add to a more favourable reaction outcome. Starting materials **1g** carrying a methoxyphenyl substituent as well as 2-thienyl substituted **1h** proved to be very reactive requiring only low reaction temperature, however, the respective products **2g** and **2h** were only formed as racemates. A control experiment confirmed that enantiopure **2g** does not racemise under the reaction conditions excluding racemisation after product formation. Seemingly, when electron-rich aryl rings are connected to the alkene, stereoselectivity of the cyclization is lost. Considering that methyl-substituted **1b** was cyclized with excellent selectivity while methoxy-substituted showed no selectivity at all, this significant difference might indicate a mechanistic cross-over. Alkenes carrying alkyl, alkenyl or alkynyl substituents were cyclized in general in good yield and with high enantioselectivity. Alkyl substituted **1i** to **1k** reacted under standard conditions to give the products in excellent enantioselectivity (95:5 or 96:4 *er*, respectively). Dienes, i.e. alkenyl-substituted starting materials **1l** and **1m**, were more reactive and required an adjustment of reaction temperature, but provided the products also in good yield and enantioselectivity. Alkynyl-containing **1o** – **1q** were less reactive and were reacted at 60 °C with slightly higher catalyst loading and longer reaction times to provide the products **1o** – **2q** in acceptable yields (54-60%) and, again, excellent enantioselectivity was observed. Monosubstituted alkene **1n** was even less reactive and despite reaction at 60 °C and a long reaction time (7 d) only partial conversion was obtained. Product **2n** was only obtained in low yield (27%) and with limited enantioselectivity (63:37 *er*).



Aryl substituents:



Alkyl and alkenyl substituents:

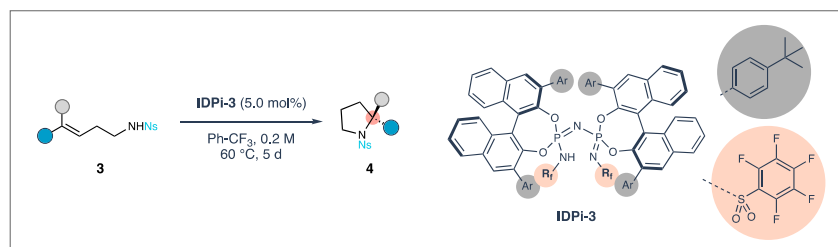


Scheme 1: Substrate scope for hydroamination of 1,1-disubstituted alkenes.

Reaction Conditions: **1** (0.3 mmol), **IDP-3** (0.006 mmol) in toluene (1.5 mL) at the mentioned temperature under argon atmosphere for 3 days. [#]Large-scale (3.6 mmol scale) experiment. ^aAfter recrystallization. [§]Using 5.0 mol% **IDP-3**. [†]Using 3.0 mol% **IDP-3**.

The reaction is scalable and cyclization of 1.2 g of **1a** provided the product **2a** in almost identical yield and with identical enantioselectivity than on smaller scale. Most products **2** are crystalline and crystallisation of **2a**, **2b** and **2k** provided crystalline materials of very high enantiopurity (> 99.5:0.5 *er*) suitable for X-ray crystallography. Based on the crystal structures of all three compounds, catalyst IDPi-3 based on (*R*)-BINOL is providing products with *R*-configuration.

Intramolecular hydroamination of trisubstituted alkenes



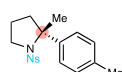
Aryl substituents:



2a
82%, 92:8 *er*
22%, 75:25 *er**



4b
83%, 92:8 *er*



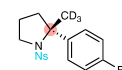
2b
76%, 80:20 *er*
40 °C, 7 d



4d
60%, 82:18 *er*
40 °C, 7 d



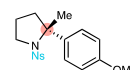
2c
75%, 77:23 *er*
7 d



4f
75%, 87:13 *er*
7 d



4g
14%, 68:32 *er*

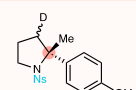


4h
85%, 50:50 *er*
1 d

Deuterium labelling experiment:



6a
78%, >95:5 *dr*
92:8 *er*



6b
80%, 50:50 *dr*
50:50 *er*
1 d

Scheme 2: Substrate scope for hydroamination of trisubstituted alkenes **3**.

Reaction Conditions: **3** (0.2 mmol) and **IDPi-3** (0.01 mmol) in trifluoromethylbenzene (1 mL) at the mentioned temperature under argon atmosphere for 5 days. * Using (*Z*)-**3a** as starting material. Reaction conditions for cyclization of labelled starting materials: **5** (0.1 mmol) and **IDPi-3** (0.005 mmol) in 0.5 mL trifluoromethylbenzene at 60 °C under argon atmosphere for 5 days.

After obtaining good yield and excellent enantioselectivity for the preparation of α,α' -disubstituted pyrrolidines from 1,1-disubstituted alkenes, the cyclization of “challenging-to-cyclize” trisubstituted alkenes was investigated. When **1** was extended by an additional methyl group to give a 5-phenylhex-5-ene-type starting material, which was supposed to undergo 5-*exo* cyclization, very low reactivity was observed (see supporting information). Instead, the 5-*endo* cyclization of (*E*)-4-phenyl-pent-4-ene derivatives **3a** was investigated (Scheme 2). This starting material proved less reactive than **1a** and required small changes in reaction conditions (60 °C, Ph-CF₃ as solvent; for details see supporting information), but ultimately underwent 5-*endo* cyclization to **2a** in good yield (82%) and in high enantioselectivity (92:8 *er*). Different substituents at the *para*-position of the phenyl group such as a methyl- or a fluoro- substituent had only a minor influence on the cyclization and products were obtained in good yield and with good enantioselectivity. Only the electron-rich methoxyphenyl substituent caused again a complete loss of enantioselectivity during the cyclization. While substitution of the methyl group on the

alkene by a trideuteromethyl had also only a minor influence on the reaction outcome (but at least in the case of **4f** an improved selectivity compared to **2f** was observed), a replacement of the methyl by an ethyl group had a very strong effect and cyclization became very slow leading to low conversion and formation of product **4g** in only 14% yield and with low enantioselectivity (68:32 *er*). When comparing the 5-*exo* cyclization of **1a** to the 5-*endo* cyclization of **3a**, both leading to product **2a**, it became clear that stereoselectivity under identical reaction conditions was not identical as might be expected if the reaction took place via a common cationic intermediate. Therefore, cyclization of (*Z*)-configured starting material (*Z*)-**3a** potentially also proceeding via the same intermediate cation was studied, however, (*Z*)-**3a** proved to be not very reactive and provided **2a** in only 22% yield and with significantly lower enantioselectivity (75:25 *er*) than via the two other pathways.

Mechanistic investigations

The surprising loss of any observed enantioselectivity for substrates carrying electron-rich aromatic substituents suggested a potential switch in mechanism when moving from standard substrates to an alkene with highly electron-rich substituents. To obtain a better understanding of the stereochemical course of the reaction (and therefore the mechanism), deuterated trisubstituted alkene **5a** was prepared. Upon cyclization under standard conditions for trisubstituted alkenes, deuterated product **6a** was obtained with excellent diastereoselectivity (95:5 *dr*; Scheme 2). Considering the diastereomeric purity of the starting material (~ 95:5 *E:Z*), the reaction proceeded stereospecifically. Based on NMR analysis, the main diastereomer was identified as **6a** proving the *anti*-addition of the proton and the sulfonamide nucleophile to the alkene. Such a highly diastereoselective *anti*-addition is unexpected for a Brønsted acid-catalyzed reaction, which is usually thought to proceed via a carbocationic intermediate. While the high diastereoselectivity could be explained by the formation of a tight ion pair in the confined space of the catalytic pocket, preventing rotation of the cationic intermediate and subsequently leading to a fast collapse and diastereoselective addition of the nucleophile, such a scenario would more likely lead to *syn*-addition. Instead, the observed *anti*-addition implies a concerted mechanism, a scenario more plausible considering the non-polar reaction medium (toluene). The complete loss of stereoselectivity when an electron-rich aryl group is present at the alkene (see **2g**, **2h** and **4h**) suggest a change in reaction mechanism for these starting materials from a concerted addition to a reaction via a free cation. To investigate this deuterium-labelled starting material **5b** carrying a methoxyphenyl-substituent was prepared. Cyclization under standard conditions proceed rapidly and provided racemic product **6b** in good yield (80%) as a 50:50 mixtures of two diastereomers (as inferred from ²H-NMR). The equimolar presence of the two diastereoisomers is in line with a reaction via a free carbocation, however, the complete absence of any diastereo- or enantioselectivity is surprising if the reaction would take place in the cavity of catalyst **IDPi-3**. One would assume that at least some minor selectivity could be observed if the reaction would proceed via a tight ion pair, but this seems to be not the case.

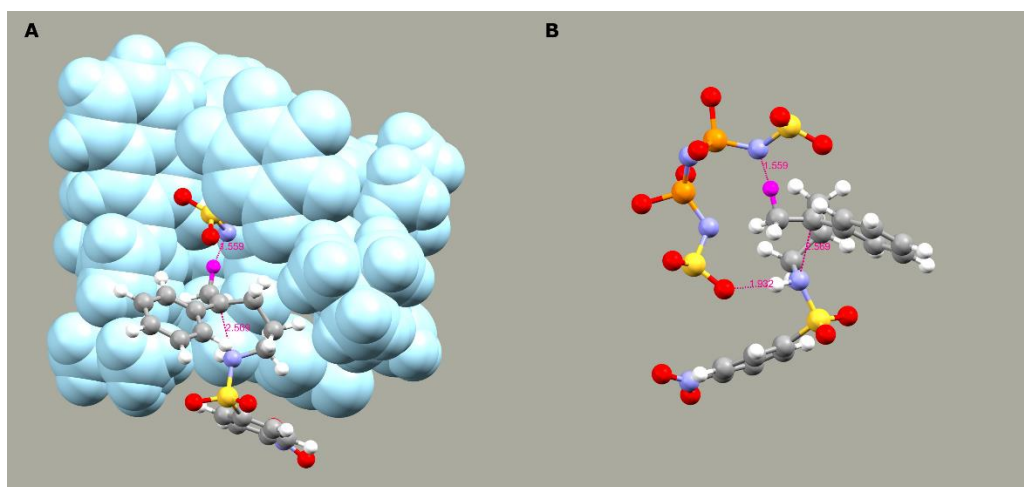


Figure 2: Calculated transition state for the anti-hydroamination of **1a** in the presence of **IDPi-3**. A: Transition state with the catalyst backbone shown as space filling model in cyan and the transferred proton in pink. B: Enlarged active site of the catalyst (backbone not shown) with key distances between substrate and catalyst depicted by pink lines (distances in Å).

To gain further insight into the mechanism, quantum chemical calculations on the reaction of **1a** to **2a** catalyzed by **IDP-3** were carried out. Due to the size of the catalyst, geometry optimizations were performed using Grimme's GFN1-xTB method (DFTB).²⁷ The calculations revealed a plausible transition state for the addition to the alkene (Figure 2) showing the experimentally observed *anti*-relationship during the addition of the proton and the nosylamide nucleophile to the alkene. The NH-proton of the nosyl-group is H-bonded to the catalyst via one of the catalyst's SO₂-groups suggesting that this group is initially accepting the proton of the nucleophile after the addition. An IRC analysis confirmed the transition state to be associated with a concerted reaction that starts from the catalyst-substrate complex and yields the cyclization product. The identity of the located TS, as well as the catalysts-substrate complex and product were confirmed by frequency calculations both at the GFN1-xTB level of theory as well as the ω B97XD/def2SVP level of theory (see supporting information).^{28,29} Electronic energies were obtained through single-point calculations of the relevant stationary points at the ω B97XD/def2TZVP level of theory and accompanied by the Gibbs free energy correction at the ω B97XD/def2SVP level of theory resulting in a Gibbs free energy of activation of 13.9 kcal/mol.

In the next step, the kinetic behaviour of the cyclization reaction of standard substrate **1a** was studied using NMR spectroscopy. Apparent rate constants k_{obs} were determined by following the decay of the ¹H-NMR signals of the starting material and rise of the signals of the product (see Figure 3A and 3B). The obtained k_{obs} agreed very well demonstrating a clean conversion without the formation of an intermediate. Apparent rate constants obtained at different temperatures were plotted against temperature and fitted to the Arrhenius equation to obtain the activation energy E_a , which was equal to 15.4 kcal/mol (Figure 3C). While this activation energy is not directly related to the Gibbs free energy of activation obtained by computational chemistry, it has to be noted that both values are quite similar and appear rather low. The results from computational chemistry suggested the formation of a rather stable complex between the starting material and the catalyst, with the starting material bound in a rather tight binding pocket similar to an enzyme. Based on this idea, initial reaction velocities at different substrate concentrations were determined at 313 K, plotted, and analysed using the Michaelis-Menten equation (Figure 3D). The data provided a good fit proving a k_{cat} value of 1.8 h⁻¹ and a K_M of 0.12 M.

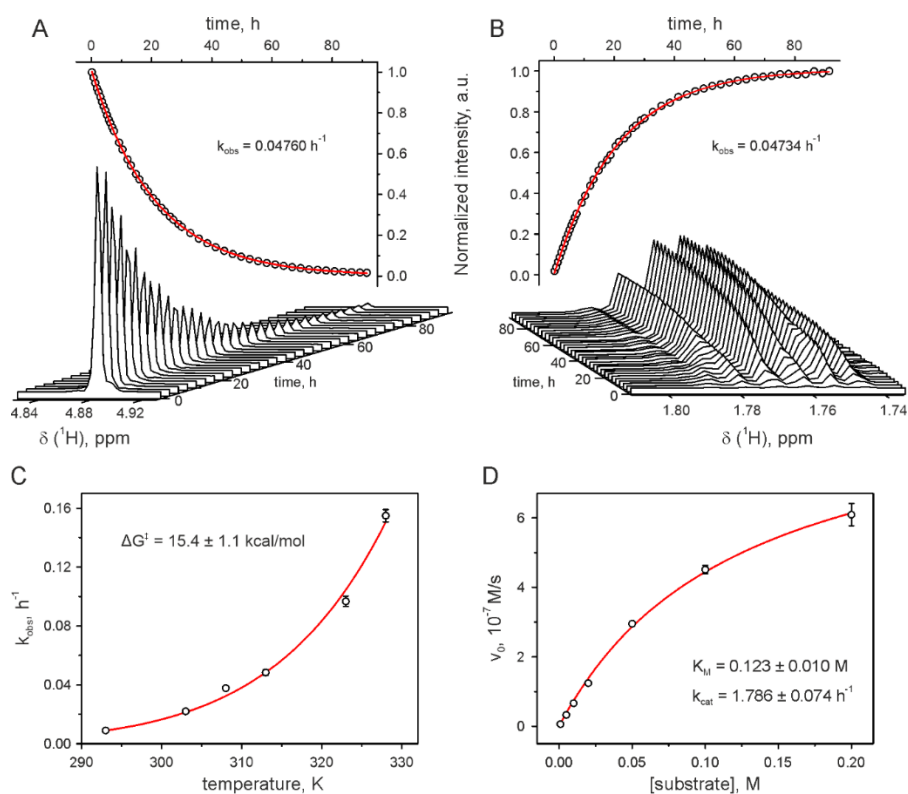
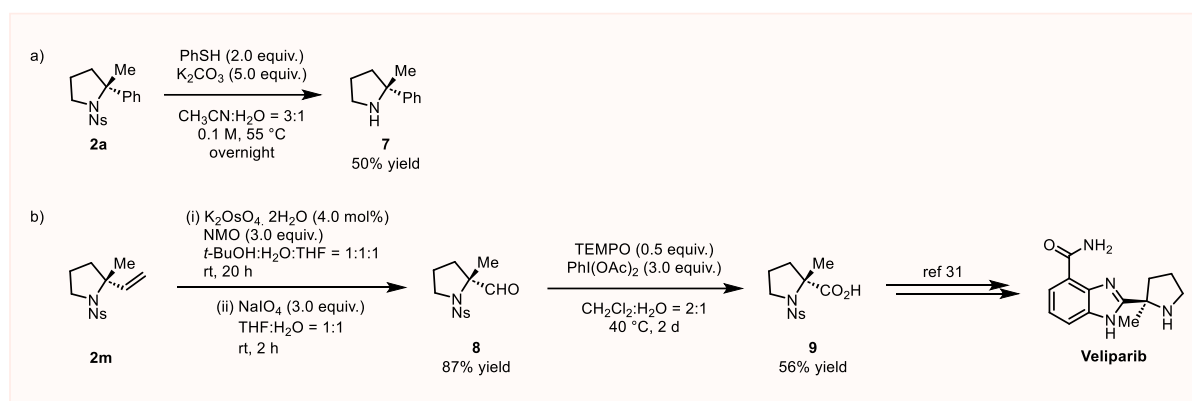


Figure 3. Kinetic analysis of the IDPi-catalyzed hydroamination reaction. (A, B) Time-dependent changes of the $1D^1H$ NMR signals of (A) the substrate **1a** proton B and (B) product **2** proton B1. The reaction was carried out in D_8 -toluene at 313 K, the catalyst concentration of 0.0067 M, and a starting substrate concentration of 0.133 M. The plots show the signal intensities (obtained by integrating the peak areas and normalized by the highest value) as a function of time. The red curves are the best fits for exponential (A) decay and (B) growth functions (see Materials and Methods), with the values of the apparent first-order rate constant (k_{obs}) indicated in the plots. (C) Arrhenius plot of k_{obs} as a function of temperature. The red curve is the best fit to the Arrhenius equation, with the value of the activation energy indicated in the plot. (D) Michaelis-Menten kinetics analysis of the initial velocity as a function of substrate concentration at 313 K and the constant catalyst concentration of 0.002 M. The red curve is the best fit to the Michaelis-Menten equation, with the K_M and k_{cat} values indicated in the plot.

Overall, the results from different methods are in good agreement with each other and suggest an enzyme-like behaviour of the **IDPi-3** catalyst. After an initial formation of a catalyst-substrate complex, hydroamination occurs via an *anti*-selective addition of the proton (electrophile) and the sulfonamide (nucleophile) in a concerted fashion. The calculated Gibbs free energy of activation would suggest a quite fast reaction; however, the Michaelis-Menten type behaviour shows a very high K_M (123 mM) for the reaction, meaning that the catalyst-substrate complex is very weak limiting the overall reaction efficiency. For the related hydroxylactonization of alkenes, List has proposed an “asynchronous-concerted” mechanism with the protonation of the alkene preceding nucleophile addition/cyclization, however, an explicit anti-addition has not been mentioned. In the current case, the high diastereoselectivity observed in the deuterium-labelling experiment and the quantum chemical calculations favour a fully concerted. Addition, at least as long as the alkene is not carrying an electron-rich aryl group.



Scheme 3: Synthetic transformations of compounds **2**.

Synthetic transformation

Compound **2a** can be deprotected under standard deprotection conditions for nosyl-groups providing free amine **7** in acceptable yield (50% yield, unoptimized; Scheme 3). Furthermore, vinyl-substituted compound **2m**, which can be easily obtained from myrcene as sustainable starting material for the synthesis of **1m** (see supporting information) followed by hydroamination, can serve as a versatile building block for the synthesis of 2-methyl proline and active pharmaceutical ingredients derived from it. The alkene in **2m** can be cleaved by bishydroxylation/diol cleavage to give aldehyde **8**, which subsequently can be oxidised to protected 2-methyl proline **9**, the key starting material for the synthesis of various PARP inhibitors such as veliparib.

Conclusions

Asymmetric Brønsted acid catalysis using highly acidic acids such as IDPis can be used for highly enantioselective hydroaminations to produce pharmaceutically-relevant pyrrolidines. Careful selection of a highly electron-deficient protecting group on nitrogen enabled efficient catalysis and avoided deactivation of the Brønsted acid catalyst by deprotonation. The reaction showcases a high substrate generality not only including di-

, but also selected trisubstituted alkenes, which are usually unreactive in IDPi catalysis. The cyclization of trisubstituted alkene enabled mechanistic investigations demonstrating that the hydroamination proceeds with very high diastereoselectivity via an *anti*-addition to the alkene. Kinetic analysis and computational investigation of the modus operandi suggests an enzyme-like behaviour of the catalyst including an initial formation of a catalyst-substrate complex prior to the concerted intramolecular cyclization.

References

1. Olivier, W. J., Smith, J. A. & Bissember, A. C. Synthesis of Pyrrolidine- and γ -Lactam-Containing Natural Products and Related Compounds from Pyrrole Scaffolds. *Chem. Rec.* **22**, e202100277 (2022).
2. Petri, G. L., Raimondi, M. V., Spanò, V.; Holl, R. Barraja, P. & Montalbano, A. Pyrrolidine in Drug Discovery: A Versatile Scaffold for Novel Biologically Active Compounds. *Top. Curr. Chem.* **379**, 34 (2021).
3. Lovering, F., Bikker, J. & Humblet, C. Escape from Flatland: Increasing Saturation as an Approach to Improving Clinical Success. *J. Med. Chem.* **52**, 6752-6756 (2009).
4. Vitaku, E., Smith, D. T. & Njardarson, J. T. Analysis of the Structural Diversity, Substitution Patterns, and Frequency of Nitrogen Heterocycles among U.S. FDA Approved Pharmaceuticals. *J. Med. Chem.* **57**, 10257-10274 (2014).
5. Mukherjee, S., Yang, J. W., Hoffmann, S. & List, B. Asymmetric Enamine Catalysis. *Chem. Rev.* **107**, 5471-5569, (2007).
6. Yadav, G. D., Chaudhary, P., Pani, B. & Singh, S. Pyrrolidine-based C1-symmetric chiral transition metal complexes as catalysts in the asymmetric organic transformations. *Tetrahedron Lett.* **134**, 154835 (2024).
7. Han, M.-Y., Jia, J.-Y. & Wang, W. Recent advances in organocatalytic asymmetric synthesis of polysubstituted pyrrolidines. *Tetrahedron Lett.* **55**, 784-794 (2014).
8. Huang, L., Arndt, M., Gooßen, K., Heydt, H. & Gooßen, L. J. Late Transition Metal-Catalyzed hydroamination and Hydroamidation. *Chem. Rev.* **115**, 2596-2697 (2015).
9. Reznichenko, A. L. & Hultsch, K. C. Hydroamination of Alkenes. *Org. React.* **88**, 1-554, (2016).
10. Kemper, J. & Studer, A. Stable Reagents for the Generation of N-Centered Radicals: Hydroamination of Norbornene. *Angew. Chem. Int. Ed.* **44**, 4914-4917 (2005).
11. Nguyen, T. M. & Nicewicz, D. A. Anti-Markovnikov Hydroamination of Alkenes Catalyzed by an Organic Photoredox System. *J. Am. Chem. Soc.* **135**, 9588-9591 (2013).
12. Musacchio, A. J., Lainhart, B. C., Zhang, X., Naguib, S. G., Sherwood, T. C. & Knowles, R. R. Catalytic intermolecular hydroaminations of unactivated olefins with secondary alkyl amines. *Science* **355**, 727-730 (2017).
13. Schlummer, B. & Hartwig, J. F. Brønsted Acid-Catalyzed Intramolecular Hydroamination of Protected Alkenylamines. Synthesis of Pyrrolidines and Piperidines. *Org. Lett.* **4**, 1471-1474 (2002).
14. Anderson, L. L., Arnold, J. & Bergman, R. G. Proton-Catalyzed Hydroamination and Hydroarylation Reactions of Anilines and Alkenes: A Dramatic Effect of Counteranions on Reaction Efficiency. *J. Am. Chem. Soc.* **127**, 14542-14543 (2005).
15. Roos, C. B., Demaerel, J., Graff, D. E. & Knowles, R. R. Enantioselective Hydroamination of Alkenes with Sulfonamides Enabled by Proton-Coupled Electron Transfer. *J. Am. Chem. Soc.* **142**, 5974-5979 (2020).
16. Brown, A. R., Uyeda, C., Brotherton, C. A. & Jacobsen, E. N. Enantioselective Thiourea-Catalyzed Intramolecular Cope-Type Hydroamination. *J. Am. Chem. Soc.* **135**, 6747-6749 (2013).
17. Shapiro, N. D., Rauniyar, V., Hamilton, G. L., Wu, J. & Toste, F. D. Asymmetric additions to dienes catalysed by a dithiophosphoric acid. *Nature* **470**, 245-250 (2011).
18. Lin, J. S., Li, T. T., Jiao, G. Y., Gu, Q. S., Cheng, J. T., Lv, L. & Liu, X. Y. Chiral Brønsted Acid-Catalyzed Dynamic Kinetic Asymmetric Hydroamination of Racemic Allenes and Asymmetric Hydroamination of Dienes. *Angew. Chem., Int. Ed.* **58**, 7092-7096 (2019).
19. Ackermann, L. & Althammer, A. Phosphoric Acid Diesters as Efficient Catalysts for Hydroaminations of Nonactivated Alkenes and Application to Asymmetric Hydroaminations. *Synlett* **7**, 995-998 (2008).
20. Lin, J. S., Yu, P., Zhang, H.P., Tan, B. & Liu, X. Y. Brønsted Acid Catalyzed Asymmetric Hydroamination of Alkenes: Synthesis of Pyrrolidines Bearing a Tetrasubstituted Carbon Stereocenter. *Angew. Chem. Int. Ed.* **54**, 7847-7851, (2015).
21. Yu, Z. L., Cheng, Y. F., Jiang, N. C., Wang, J., Fan, L. W., Yuan, Y., Li, Z. L., Gu, Q. S. & Liu, X. Y. Desymmetrization of unactivated bis-alkenes via chiral Brønsted acid-catalysed hydroamination. *Chem. Sci.* **11**, 5987-5993, (2020).

22. Takagi, R., Duong, D. T. & Ichiki, T. Disulfonimide catalyzed asymmetric intramolecular hydroamination of alkenyl thioureas: Concentration effect in the hydroamination. *Tetrahedron* **94**, 132332 (2021).
23. Jung, M. E. & Piizzi, G. *gem*-Disubstituent Effect: Theoretical Basis and Synthetic Applications. *Chem. Rev.* **105**, 1735-1766 (2005).
24. Čorić, I. & List, B. Asymmetric spiroacetalization catalysed by confined Brønsted acids. *Nature* **483**, 315-319 (2012).
25. Schreyer, L., Properzi, R. & List, B. IDPi Catalysis. *Angew. Chem., Int. Ed.* **58**, 12761-12777 (2019).
26. Tsuji, N., Kennemur, J. L., Buyck, T., Lee, S., Prévost, S., Kaib, P. S. J., Bykov, D., Farès, C. & List, B. Activation of olefins via asymmetric Brønsted acid catalysis. *Science* **359**, 1501-1505 (2018).
27. Grimme, S., Bannwarth, C. & Shushkov, P. A Robust and Accurate Tight-Binding Quantum Chemical Method for Structures, Vibrational Frequencies, and Noncovalent Interactions of Large Molecular Systems Parametrized for All spd-Block Elements ($Z = 1-86$). *J. Chem. Theory Comput.* **13**, 1989-2009 (2017).
28. Chai, J.-D. & Head-Gordon, M. Long-range corrected hybrid density functionals with damped atom-atom dispersion corrections. *Phys. Chem. Chem. Phys.* **10**, 6615-6620 (2008).
29. Weigend, F. & Ahlrichs, R. Balanced basis sets of split valence, triple zeta valence and quadruple zeta valence quality for H to Rn: Design and assessment of accuracy. *Phys. Chem. Chem. Phys.* **7**, 3297-3305 (2005).
30. Maji, R., Ghosh, S., Grossmann, O., Zhang, P., Leutzsch, M., Tsuji, N. & List, B. A Catalytic Asymmetric Hydroxylactonization. *J. Am. Chem. Soc.* **145**, 8788-8793 (2023).
31. Kolaczowski, L., Barkalow, J., Barnes, D. M., Haight, A., Pritts, W. & Schellinger, A. Synthesis of (*R*)-Boc-2-methylproline via a Memory of Chirality Cyclization. Application to the Synthesis of Veliparib, a Poly (ADP-ribose) Polymerase Inhibitor. *J. Org. Chem.* **84**, 4837-4845 (2019).

Acknowledgements

U.H. is grateful for the financial support by VUB grant OCR 3327. Debbie Mangelings and Christine Duverger (VUB) is thanked for additional MS measurement.

Author contributions

S.G and U.H. conceived the project, analysed the results and wrote the paper with the input of all authors. S.G. conducted most of the synthetic experiments including the synthesis of starting materials and catalysts and the development of the reaction. R.K. contributed to catalyst and starting material synthesis as well as reaction development. A.N.V. carried out kinetic experiments by NMR and analysed the kinetic data. R.V.L. and F.D.P. designed and carried out the DFT calculations. C.G.D. carried out crystal structure determinations by X-ray analysis.

Competing interests

The authors declare no competing interests.